Chemical Engineering Journal 149 (2009) 78–86

Contents lists available at ScienceDirect

Chemical Engineering Journal

journal homepage: www.elsevier.com/locate/cej

Relevance of hindrance factors and hydrodynamic pressure gradient in the modelization of the transport of neutral solutes across nanofiltration membranes

V. Silva, P. Prádanos*, L. Palacio, J.I. Calvo, A. Hernández

Grupo de Superficies y Materiales Porosos (SMAP), Dpto. de Física Aplicada, Facultad de Ciencias,
Universidad de Valladolid, Valladolid, Spain

ARTICLE INFO

Article history:
Received 31 July 2008
Received in revised form
23 September 2008
Accepted 1 October 2008

Keywords:
Nanofiltration
Applied pressure
Pore-wall friction
Hindrance factors
Transport model

ABSTRACT

Here we show how the usual model for the transport of neutral solutes through porous membranes, lead to equations that can be compared with the thermodynamic equations of transport. This is done in detail and paying special attention to the assumptions made that frequently have been not taken into account.

This model can be used to get information on the pore size from functional data on retention and permeability. Two parameters are needed to fit experimental results of retention versus volume flow. We show the total equivalence of using the Staverman reflection coefficient and the solute permeability coefficient as parameters or the pore radius and the ratio of porosity and pore length. It is also equivalent to measure, adequate and separately, the reflection and the permeability coefficients and to evaluate from them the pore radius and the ratio of porosity versus pore length or vice versa. Moreover, the effect of the amplification of viscosity in small pores and the information contained in the pure water permeability are included in the model to reduce the number of required parameters to one, as for example the pore radius.

We show that when the pore reflection coefficient is considered some bounds for the values of the pore hindrance factors must be accomplished for big and small molecules as compared to the pore size. Criteria to allow an election among the many expressions proposed for such hindrance factors in literature are proposed based on these requirements. An adequate consideration of pore wall friction and applied pressure gradient is shown to be very important as far as when these factors are inappropriately neglected, very significant errors appear in the prediction of performances of nanofiltration membranes, mainly for intermediate retentions.

1. Introduction

Membranes are barriers that are selective to one or several components of a feed mixture, generally a solution, to be separated from the rest of their constituents. Nanofiltration (NF) is a membrane separation process where size exclusion in the range of the nanometer happens. This process is actually in between Ultrafiltration (UF) and Reverse Osmosis (RO). Actually, apart from the size exclusion mechanism, rejection in these systems is also influenced by the charge in the membrane pores. This is the reason why most of the NF membranes are highly effective in the ionic separation due to the electrostatic repulsion. This also allows working at lower pressures than for RO, normally in the range 0.3 and 1.4 MPa. In summary, NF membranes allow high fluxes, high rejection values for salts with multivalent ions, a low molecular weight cut-off (between 200 and 2000 Da) for non-charged substances. The inversion, operation and maintenance costs are also relatively low for nanofiltration [1,2].

The first generation of NF membranes dates back to 1970. Then a new kind of RO membranes, allowing a reasonable flux of water at relatively low pressures, were developed. This allowed a substantial decrease in operation costs as compared with the traditional RO membranes. These new membranes were called nanofiltration membranes, being totally established in 1980 when the first applications started to be published [2]. The application and knowledge of Nanofiltration technology has enlarged quickly in the last years [3]. Nowadays, it is applied basically to the salt rejection in water treatment and in fractionation of salts and small molecules in a great number of industries [4] as: removal of pesticides in subterranean waters, removal of heavy metals from

---

* Corresponding author. Tel.: +34 983423739; fax: +34 983423136.
E-mail address: pradanos@termo.uva.es (P. Prádanos).

1385-8947/$ – see front matter © 2008 Elsevier B.V. All rights reserved.
doi:10.1016/j.cej.2008.10.002

Nomenclature

A_k	porosity
c	molar concentration inside the membrane (mol/m^3)
d_w	thickness of the solution layer (m)
D	diffusion coefficient (m^2/s)
D_p	diffusivity inside the membrane (m^2/s)
f_{ij}	friction coefficients of i with j (J s/mol m^2)
f,g	wall correction factors for diffusion and filtration flow
G,K^{-1}	hydrodynamic coefficients
J_s,j_s	solute molar flux (mol/m^{2}s)
J_V,j_V	volumetric flux (m/s)
K_c	hindrance factor for convection
$K_c{}'$	hindrance factor for convection with pressure gradient effect
K_d	hindrance factor for diffusion
L_{pw}	water permeability (m/s Pa)
M	molecular weight (kg/mol)
N_a	Avogadro number (1/mol)
P	pressure (N/m^2)
ΔP	applied pressure (Pa)
Pe	Peclet number
r	pore radius (m)
r_s	stokes radius (m)
r_p	effective pore radius (m)
R	gas constant (J/mol K)
R_s	solute retention
$R_s{}'$	solute retention with pressure gradient effect
S_D,S_F	steric hindrance factor for diffusion and filtration flow
T	temperature (K)
$\bar{V}_i$	molar partial volume of the i-th solute (m^3/mol)
x	axial position in the membrane (m)
Δx	membrane thickness (m)

Greek symbols

Φ	steric partition coefficient
χ	molar fraction
γ	activity coefficient
η	solvent viscosity in the pores (Pa s)
η_0	bulk solvent viscosity (Pa s)
λ	solute radius/ pore radius
μ	chemical potential (J/mol)
υ	velocity (m/s)
$\Delta\pi$	Osmotic pressure difference (Pa)
ρ	density (kg/m^3)
σ	reflection coefficient
ω	solute permeability (mol/m^2 s Pa)

Subindex

m	membrane
p	pore
s	solute
w	water

Superindex

0	bulk
*	pure water

waste-water, recycling of waste-water from industrial washing processes, water softening and removal of nitrates, among others.

The mechanisms involved in nanofiltration [5], are different for the charged and uncharged membranes, or equivalently for ions in solution (dissolved salts) and uncharged solutes (organic compounds). The differences are attributable to the presence or absence of relevant electrostatic interactions. In all cases size exclusion and convection are present. In case of uncharged solutes, rejection appears only by a mechanism of convection combined with diffusion in the nanoporous structure, which depends also on the molecular size. In the case of charged species other parameters have to be considered as the volumetric charge density, χ and the dielectric constants both inside the pores, ε_{p}, and in the solid membrane material, ε_{m}, when dielectric exclusion is significant [4,6–9]. Experiments of separation of organic molecules, thus in conditions of steric hindrance, convection and diffusion, are crucial to characterize the porous structure of nanofiltration membranes.

In the case of uncharged solutes, rejection appears only by a mechanism of convection modulated by differences in the diffusivities in the nanoporous structure [10]. For pure steric hindrance and for the sorption-diffusion mechanism, the actual pore size distribution plays a key part thus it should be taken into account for the separation of organic molecules [11]. Simulations assuming log normal pore size distributions show that retention decreases quickly by assuming wider pore size distributions [12]. The possible variation of the pore section along a pore has also recently been taken into account [13].

Here a study of the detailed mechanisms involved in rejection and transport of uncharged species through nanofiltration membranes are presented. Here we will also assume that pores are all equal in size and shape with a uniform section. The applied pressure gradient, that is frequently assumed to have negligible effects, is nevertheless considered here and its actual relevance is discussed in detail. Some attempts have been done to include this pressure gradient previously [12] nevertheless here we will rather follow the point of view introduced by Nakao and Kimura [14]. This approach has the advantage of introducing the action of the pressure gradient within the very well founded frame of Thermodynamics.

Nakao and Kimura [14] discussed the convenience of including or excluding the pore wall friction in the hindrance coefficients. Recently Li and co-workers [15] have analyzed this problem from an “ad hoc” point of view based on experimental results for the filtration of fructo-oligosaccharides. Here we will analyze how to include pore wall friction correctly and the different expressions for the hindrance convective and diffusive factors are compared. Criteria will be proposed to help in the process of selection of the correct correlations for the hindrance factors in accordance with their definition and their relation to thermodynamic parameters [16].

2. Transport model

Both the friction and thermodynamic models used to describe the transport of uncharged solutes through nanofiltration membranes (and actually also through ultrafiltration membranes) are described, in this section. They both depend ultimately on the ratio between membrane thickness and porosity, $\Delta x/A_{\mathrm{k}}$ and on the ratio of solute and pore radii, λ, through the so called diffusive and convective hindrance factors. The different correlations proposed in the literature for these coefficients are considered and criteria for an adequate election among them are discussed too.

2.1. Friction model

The forces on water and solute molecules are proportional to the gradient of chemical potential and assuming that the membrane is seen as quiet ($\upsilon_m = 0$) [17,18]:

$$-\frac{d\mu_w}{dx} = (f_{ws} + f_{wm})\upsilon_w - f_{ws}\upsilon_s \tag{1}$$

$$-\frac{d\mu_s}{dx} = -f_{sw}\upsilon_w + (f_{sw} + f_{sm})\upsilon_s \tag{2}$$

But, the drag force on the solute assumed to behave as a sphere moving in a also moving liquid (here water) is

$$F_{drag} = f_{sw}^0 \frac{\upsilon_s - \upsilon_w g(\lambda)}{f(\lambda)} \tag{3}$$

A comparison of these expressions for the force on the solute, Eqs. (2) and (3), leads to

$$\left.\begin{array}{l} (f_{sw} + f_{sm}) = \left[\dfrac{f_{sw}^0}{f(\lambda)}\right] \\ f_{sw} = \left[f_{sw}^0 \dfrac{g(\lambda)}{f(\lambda)}\right] \end{array}\right\} \tag{4}$$

The factors f and g account for the pore wall action on the drag force and they depend on $\lambda = r_s/r_p$ for cylindrical pores. The bulk mobility of the solute relative to water, f_{sw}^0, is

$$f_{sw}^0 = \frac{RT}{D_s} \tag{5}$$

according to the Einstein equation for non-turbulent flows. By taking into account also the Stokes equation,

$$f_{sw}^0 = 6\pi\eta r_s N_A \tag{6}$$

which is valid for spherical molecules at low Reynolds numbers. The assumption of spherical solutes is reasonably good for solute molecules not too long or soft enough to appear curled up or small enough as usually found in nanofiltration. Note that from Eqs. (5) and (6) the Stokes–Einstein equation is obtained for the diffusion coefficient, $D_s = RT/6\pi\eta r_s N_A$.On the other hand the solute chemical potential is

$$\mu_s = \mu_s^\infty(T, p = 1) = \int_1^p \bar{V}_s^\infty dp + RT\,\ln(\gamma_s \chi_s) \tag{7}$$

$\bar{V}_s^\infty$ is the molar partial volume for the solute at infinite dilution, χ_s is the molar fraction of the solute and γ_s is the coefficient of activity. For diluted solutions:

$$\left.\begin{array}{r} \gamma_s \approx 1 \\ \chi_s \approx \dfrac{M_w}{\rho_w} c_s \end{array}\right\} \tag{8}$$

and $\bar{V}_s^\infty \approx \bar{V}_s$. Note that the assumption of dilute solutions is very reasonable for highly retaining membranes with not too highly concentrated solutions as usually encountered in nanofiltration. [19]. Then, after differentiation:

$$-\frac{d\mu_s}{dx} = -\bar{V}_s \frac{dp}{dx} - \frac{RT}{c_s}\frac{dc_s}{dx} \tag{9}$$

The solute flux $j_s(r) \equiv \upsilon_s(r) c_s$ is, according to Eqs. (2), (4) and (9):

$$j_s(r) = -D_s f(\lambda)\frac{dc_s}{dx} + c_s g(\lambda)\upsilon_w - \bar{V}_s \frac{D_s c_s}{RT} f(\lambda)\frac{dp}{dx} \tag{10}$$

or

$$j_s(r) = -D_s f(\lambda)\frac{dc_s}{dx} + c_s g(\lambda)\upsilon_w - \bar{V}_s \frac{c_s}{f_{sw}^0} f(\lambda)\frac{dp}{dx} \tag{11}$$

For pure water:

$$-\frac{d\mu_w^*}{dx} = f_{wm}^* \upsilon_w^* \tag{12}$$

And

$$\mu_w^* = \mu_w^*(T, p = 1) + \int_1^p V_w^*\, dp \tag{13}$$

where V_w^* is the molar volume of pure water. After differentiation and according to Eq. (12)

$$\frac{dp}{dx} = -\frac{f_{wm}^*}{V_w^*}\upsilon_w^* \Rightarrow \upsilon_w^* = -\frac{V_w^*}{f_{wm}^*}\frac{dp}{dx} \tag{14}$$

and, by taking into account the Hagen–Poiseuille equation

$$\upsilon_w^* = -\frac{r_p^2}{8\eta_w}\frac{dp}{dx} \tag{15}$$

And thus

$$\frac{V_w^*}{f_{wm}^*} = \frac{r_p^2}{8\eta_w} \tag{16}$$

Then, according to Eqs. (15) and (16), Eq. (11) is:

$$j_s(r) = -D_s f(\lambda)\frac{dc_s}{dx} + c_s\left[g(\lambda)\upsilon_w + \frac{\bar{V}_s}{f_{sw}^0 V_w^*} f(\lambda) f_{wm}^* \upsilon_w^*\right] \tag{17}$$

But $f_{wm}\upsilon_w \approx f_{wm}^*\upsilon_w^*$ for dilute solutions as far as, according to Eq. (1)

$$-\frac{d\mu_w}{dx} = f_{ws}(\upsilon_w - \upsilon_s) + f_{wm}\upsilon_w \tag{18}$$

Due to the action–reaction balance of friction forces

$$f_{ws} = \frac{c_s}{c_w} f_{sw} \tag{19}$$

Therefore, by the second Eq. (4):

$$f_{ws} = \frac{c_s}{c_w}\left[f_{sw}^0 \frac{g(\lambda)}{f(\lambda)}\right] \tag{20}$$

Given that we deal with diluted solutions

$$\frac{c_s}{c_w} \to 0 \tag{21}$$

and thus, $f_{ws} \approx 0$. Then, according to Eq. (18),

$$-\frac{d\mu_w}{dx} \approx f_{wm}\upsilon_w \tag{22}$$

and for diluted solutions:

$$\frac{d\mu_w}{dx} \approx \frac{d\mu_w^*}{dx} \Rightarrow f_{wm}\upsilon_w \approx f_{wm}^*\upsilon_w^* \tag{23}$$

where Eqs. (12) and (22) have been taken into account. Then Eq. (17) reads:

$$j_s(r) = -D_s f(\lambda)\frac{dc_s}{dx} + c_s\left[g(\lambda) + \frac{f_{wm}\bar{V}_s}{f_{sw}^0 V_w^*} f(\lambda)\right]\upsilon_w \tag{24}$$

For spherical solutes

$$\bar{V}_s = N_A \frac{4}{3}\pi r_s^3 \tag{25}$$

Then also using Eqs. (6) and (16) (assuming that $\eta_w \approx \eta$ again because the solution is diluted) [14]

$$\frac{f_{wm}\bar{V}_s}{f_{sw}^0 V_w^*} = \frac{16}{9}\lambda^2 \tag{26}$$

It has also been accepted that for diluted solutions $f_{wm} \approx f_{wm}^*$ [20], because $\upsilon_w^* \approx \upsilon_w$ (see Eq. (23)). In this way Eq. (24) is:

$$j_s(r) = -D_s f(\lambda)\frac{dc_s}{dx} + c_s\left[g(\lambda) + \frac{16\lambda^2}{9} f(\lambda)\right]\upsilon_w \tag{27}$$

If laminar flow inside a cylindrical pore is totally developed, the water velocity acquires a parabolic profile

$$\upsilon_w = \upsilon_w^c\left[1 - \left(\frac{r}{r_p}\right)^2\right] = \upsilon_w^c(1-\lambda^2) \tag{28}$$

where υ_w^c is the maximal velocity of water in the profile which happens in the centerline ($r=0$). Assuming that the center of the spherical molecules of solute can be placed equally distributed inside a circle of radius r_p–r_s as far as when a solute molecule touches the pore walls its center is placed at a distance r_s from the wall, thus the $j_s(r)$ averaged for all the possible values of the radial coordinate is [21]

$$\left\langle j_s\right\rangle = \frac{1}{\pi r_p^2}\int_0^{r_p-r_s} j_s(r)2\pi r\,dr = f(\lambda)\int_0^{r_p-r_s}\left\{-D_s\frac{dc_s}{dx} + c_s \left[\frac{g(\lambda)}{f(\lambda)} + \frac{16\lambda^2}{9}\right]\upsilon_w^c\left[1-\left(\frac{r}{r_p}\right)^2\right]\right\}2\pi r\,dr \tag{29}$$

and

$$\left\langle j_s\right\rangle = -\left(1-\frac{r_s}{r_p}\right)^2 f(\lambda)D_s\frac{dc_s}{dx} + c_s f(\lambda)\left[\frac{g(\lambda)}{f(\lambda)} + \frac{16\lambda^2}{9}\right]\upsilon_w^c\left[\left(1-\frac{r_s}{r_p}\right)^2 - \frac{1}{2}\left(1-\frac{r_s}{r_p}\right)^4\right] \tag{30}$$

It has been assumed that both f and g do not depend on the radial coordinate r.

This can be written as:

$$\left\langle j_s\right\rangle = -S_D f(\lambda)D_s\frac{dc_s}{dx} + c_s f(\lambda)\left[\frac{g(\lambda)}{f(\lambda)} + \frac{16\lambda^2}{9}\right]\frac{\upsilon_w^c}{2}S_F \tag{31}$$

With [21,14],

$$\left.\begin{aligned} S_D &= (1-\lambda)^2 \equiv \phi \\ S_F &= 2(1-\lambda)^2 - (1-\lambda)^4 = \phi(2-\phi) \end{aligned}\right\} \tag{32}$$

On the other hand the total volume flow is

$$\left\langle j_V\right\rangle = c_w\left\langle\upsilon_w\right\rangle\bar{V}_w + c_s\left\langle\upsilon_s\right\rangle\bar{V}_s \approx \left\langle\upsilon_w\right\rangle \tag{33}$$

As far as for diluted solutions:

$$\left.\begin{aligned} c_w\bar{V}_w &\approx 1 \\ c_s\bar{V}_s &\approx 0 \end{aligned}\right\} \tag{34}$$

and by taking into account Eq. (28) the average water velocity in the pore is:

$$\left\langle\upsilon_w\right\rangle = \frac{1}{\pi r_p^2}\int_0^{r_p}\upsilon_w(r)2\pi r\,dr = \frac{1}{\pi r_p^2}\int_0^{r_p}\upsilon_w^c\left[1-\left(\frac{r}{r_p}\right)^2\right]2\pi r\,dr = \frac{\upsilon_w^c}{2} \tag{35}$$

And finally correlating the fluxes per unit of pore area to those per unit of membrane area

$$J_s = \left\langle j_s\right\rangle A_k \quad\text{and}\quad J_V = \left\langle j_V\right\rangle A_k \tag{36}$$

and

$$J_s = -S_D f(\lambda)D_s A_k\frac{dc_s}{dx} + S_F c_s f(\lambda)\left[\frac{g(\lambda)}{f(\lambda)} + \frac{16\lambda^2}{9}\right]J_V \tag{37}$$

It is worth noting that the same averaging done in Eq. (29) should be done to correlate the concentration inside the pore to that existing in an unrestricted medium (as the bulk outside the pore) in equilibrium with the pore at each longitudinal coordinate, i.e.:

$$c_s^i(x) = \frac{1}{\pi r_p^2\Delta x}\int_0^{r_p-r_s} c_s(x)2\pi r\Delta x\,dr = \left(1-\frac{r_s}{r_p}\right)^2 c_s(x) = \Phi c_s(x) \tag{38}$$

where the correlation of concentrations has been called, Φ, as customarily. When there is an external field acting this partition equation should be substituted by

$$\begin{aligned} c_s^i(x) &= \frac{1}{\pi r_p^2\Delta x}\int_0^{r_p-r_s} e^{-\Delta\psi}c_s(x)2\pi r\Delta x\,dr \\ &= \left(1-\frac{r_s}{r_p}\right)^2 e^{-\Delta\psi}c_s(x) = \Phi e^{-\Delta\psi}c_s(x) \end{aligned} \tag{39}$$

$\Delta\psi$ the potential drop at pore extremes which is called Donnan potential. This form of partitioning relationship should be used, for example, for ionic solutes.

Here we assume that the solute is uncharged, then Eq. (37) reads:

$$J_s = -\Phi K_d(\lambda)D_s A_k\frac{dc_s}{dx} + \Phi K_c{}' c_s J_V \tag{40}$$

with

$$\left.\begin{aligned} &K_d \equiv f(\lambda) \\ &K_c{}' \equiv (2-\phi)f(\lambda)\left[\frac{g(\lambda)}{f(\lambda)} + \frac{16\lambda^2}{9}\right] = K_c + (2-\phi)K_d\left(\frac{16\lambda^2}{9}\right) \end{aligned}\right\} \tag{41}$$

that are called respectively diffusive and convective hindrance factors. Note that the convective hindrance factor if the pressure gradient was not taken into account should be K_c.

If the differential Eq. (40) is integrated for all the length of the pore:

$$\int_0^{\Delta x} J_s dx = J_s\Delta x = -\Phi K_d D_s A_k(c_{2s} - c_{1s}) + \Phi K_c{}' J_V\int_0^{\Delta x} c_s dx \tag{42}$$

and

$$J_s = -\Phi K_d A_k\frac{c_s(\Delta x) - c_s(0)}{\Delta x} + \Phi K_c{}' J_V\frac{1}{\Delta x}\int_0^{\Delta x} c_s\,dx \tag{43}$$

That is

$$J_s = -\Phi K_d D_s A_k\frac{\Delta c_s}{\Delta x} + \Phi K_c{}' J_V\bar{c}_s \tag{44}$$

[18], where $\bar{c}_s$ is the average concentration along the pore.

2.2. Thermodynamic equations for the transport

For such a system, according to the Thermodynamics of Irreversible Processes:

$$\left.\begin{aligned} J_v &= L_p(\Delta p - \sigma\Delta\textstyle\prod) \\ J_s &= \omega\Delta\textstyle\prod + (1-\sigma)J_v\bar{c}_s \end{aligned}\right\} \tag{45}$$

which are the so called Spiegler–Kedem–Katchalsky [19,22], equations which are valid for diluted enough solutions and give the volume and solute fluxes in terms of hydraulic and osmotic pressure differences across the membrane. The Van't Hoff equation allows an evaluation of the osmotic pressure as:

$$\prod = RTc_s \tag{46}$$

for dilute solutions. Then, the solute flux is:

$$J_S = \omega RT\Delta c_s + (1-\sigma)J_V\bar{c}s \tag{47}$$

A comparison of Eq. (47) with equation with Eq. (44) leads to

$$\left.\begin{aligned}(1-\sigma) &= \Phi K_c{}' \\ \omega &= -\Phi\frac{K_d D_s}{RT}\left(\frac{A_k}{\Delta x}\right)\end{aligned}\right\} \tag{48}$$

These equations with the values given in Eq. (41) are the basis of the so called steric hindrance pore model, SHP [14,23–25] and used frequently in more or less simplified versions.

2.3. The hindrance factors

The wall solute interaction factors, *f* and *g* can be evaluated by a detailed study of drag forces for different λ. The hindrance factors, *f* and *g* take into account the solute movement through confined geometries as those of the membrane pores where the transport is hindered. Many alternative expressions have been proposed for these hindrance factors all them based on the analysis of the detailed fluid mechanics of particles moving through tubes or capillaries containing a still fluid.

A review of many of these calculations was presented by Deen [26]. After the seminal works of Ferry [27], Pappenheimer et al. [28], and Renkin [29], one of the first detailed study of such *f* and *g* functions of λ for wide range of λ ($0 < \lambda \leq 0.9$) was addressed by Haberman and Sayre [30], and afterwards used by Verniory et al. [21], and Nakao and Kimura [14]. They evaluated the factors as:

$$f(\lambda) = \frac{1 - 2.105\lambda + 2.0865\lambda^3 - 1.7068\lambda^5 + 0.7260\lambda^6}{1 - 0.75857\lambda^5} \tag{49}$$

$$g(\lambda) = \frac{1 - (2/3)\lambda^2 - 0.20217\lambda^5}{1 - 0.75857\lambda^5} \tag{50}$$

Bohlin [31], derived similar equations. A complete correlation ($0 < \lambda \leq 1$) was due to Bungay and Brenner [32]:

$$f = \frac{6\pi}{K_t} \tag{51}$$

and

$$g = \frac{K_s}{2K_t} \tag{52}$$

with

$$K_t = \frac{9}{4}\pi^2\sqrt{2}(1-\lambda_t)^{-5/2}\left(1 + \sum_{n=1}^{2} a_n(1-\lambda_i)^n\right) + \sum_{n=0}^{4} a_{n+3}\lambda_i^n \tag{53}$$

$$K_s = \frac{9}{4}\pi^2\sqrt{2}(1-\lambda_t)^{-5/2}\left(1 + \sum_{n=1}^{2} b_n(1-\lambda_i)^n\right) + \sum_{n=0}^{4} b_{n+3}\lambda_i^n \tag{54}$$

where $a_1 = -73/60$; $a_2 = 77.293/50.4$; $a_3 = -22.5083$; $a_4 = -5.6117$; $a_5 = -0.3363$; $a_6 = -1.216$; $a_7 = 1.647$; $b_1 = 7/60$; $b_2 = -2.227/50.4$; $b_3 = 4.018$; $b_4 = -3.9788$; $b_5 = -1.9215$; $b_6 = 4.392$ and $b_7 = 5.006$.

Other very accurately evaluated correlations could be used, even though they are only valid for a limited range of λ, as for example:

$$f(\lambda) = 1 - 2.1044\lambda + 2.089\lambda^3 - 0.948\lambda^5 \tag{55}$$

$$g(\lambda) = 1 - \left(\frac{2}{3}\right)\lambda^2 - 0.163\lambda^3 \tag{56}$$

due to Anderson and Quinn [33], that seems to be valid for $0 \leq \lambda \leq 0.4$ or those due to Brenner and Gaydos [34]:

$$f(\lambda) = \frac{1 - (9/8)\lambda\ \ln\lambda^{-1} - 1.539\lambda)}{1 - 2\lambda + \lambda^2} \tag{57}$$

$$g(\lambda) = \frac{1 + 2\lambda - 4.9\lambda^2}{1 + 2\lambda - \lambda^2} \tag{58}$$

that has been obtained by using radial averages (instead of centerline movements) and can be used for $0 < \lambda \leq 0.1$. Or the correlation for *f*, evaluated also from radial averages, due to Mavrovouniotis and Brenner [35]:

$$f(\lambda) = \frac{0.984(1-\lambda)^{9/2}}{1 - 2\lambda + \lambda^2} \tag{59}$$

Finite elements have been used also by Bowen and Sharif [36], to analyze the movement of a spherical molecule of the solute along the centerline of a cylindrical pore to give

$$f(\lambda) = -1.705\lambda + 0.946 \tag{60}$$

$$g(\lambda) = -0.301\lambda + 1.022 \tag{61}$$

being these expressions adequate for $0 < \lambda \leq 0.4$.

Later, Bowen et al. [37], modified the procedure of calculation of the *f* and *g*, based on more detailed studies on the solute movement in cylindrical tubes to

$$f(\lambda) = 1.0 - 2.30\lambda + 1.154\lambda^2 + 0.224\lambda^3 \tag{62}$$

$$g(\lambda) = 1.0 + 0.054\lambda - 0.988\lambda^2 + 0.441\lambda^3 \tag{63}$$

the authors claimed that this expansion in λ was adequate for $0 < \lambda \leq 0.8$. Still later Bandini and Vezanni [38], proposed an extrapolation for $0.8 < \lambda \leq 1$ as

$$f(\lambda) = -0.105 + 0.318\lambda - 0.213\lambda^2 \tag{64}$$

$$g(\lambda) = -6.830 + 19.348\lambda - 12.518\lambda^2 \tag{65}$$

These correlations are shown in Figs. 1 and 2 in terms of K_d and K_c evaluated according to Eq. (41).

Some efforts have been done to extend this theoretical frame to non-spherical, non-rigid molecules [39–43]. Other averaged correlations have been proposed later as for example those due to

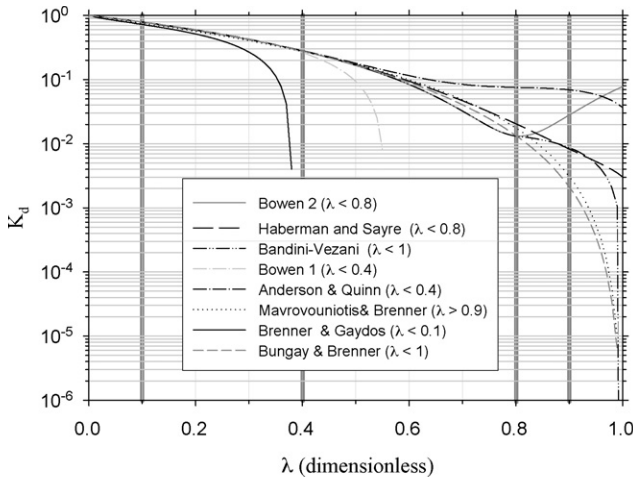

Fig. 1. Several correlations, given in the literature, for the diffusive hindrance factor as a function of $\lambda = r_s/r_p$. The range of λ that authors claim for their correlations are shown in the legend.

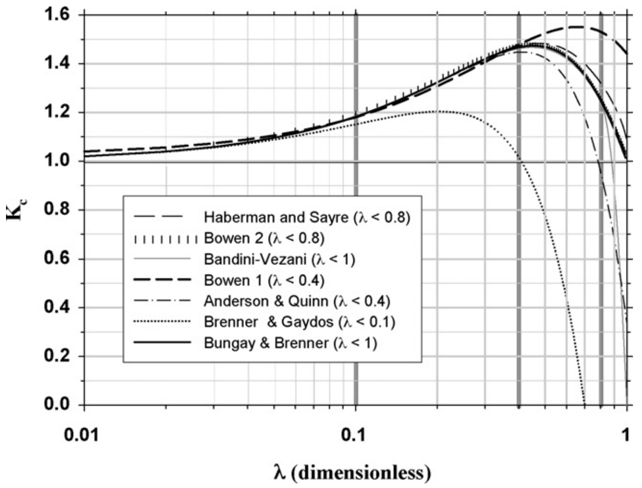

Fig. 2. Several correlations, given in the literature, for the convective hindrance factor as a function of $\lambda = r_s/r_p$. The range of λ that authors claim for their correlations are shown in the legend.

Dechadilok and Deen [44] that claim to be valid up to $\lambda < 0.9$. They are based on numerical integration of results based on an evaluation by finite elements for some discrete values of λ given by Higdon and Muldowney [45] and on approximations due to Ennis et al. [46]. The centerline approximation given by the Bungay and Brenner expressions turns to be surprisingly accurate [44].

It seems clear that both f and g should go to 1 for $\lambda \to 0$ as far as then the pore walls should play no action on the solute—see Eq. (4). On the other hand, when $\lambda \to 1$ then $f \to 0$ in order to make infinite the friction coefficients with both water and membrane, according again to Eq. (4). In this way the numerator of Eq. (3) should go to zero as the denominator does keeping finite the drag force and thus possible the movement of the solute. In these conditions the solute should move similarly to a piston and its speed along the pore centerline should approach the average of that of water in a pore section. If laminar regime is assumed this means that the solute should move along the pore centerline at half the velocity of water along the same centerline—see Eq. (35), thus $g \to 1/2$ in order to keep finite the force drag.

According to Eq. (41) the same tendencies for $\lambda \to 0$ and $\lambda \to 1$ that are shown by f and K_d hold for g and both K_c and K_c'. On the other hand, according to Eq. (48) and taking into account that

$$\left.\begin{array}{l} \lambda \to 0 \Rightarrow \Phi \to 1 \\ \lambda \to 1 \Rightarrow \Phi \to 0 \end{array}\right\} \tag{66}$$

it is clear that

$$\lambda \to 0 \left\{ \begin{array}{c} \sigma \to 0 \\ \omega \to -\dfrac{D_s}{RT}\left(\dfrac{A_k}{\Delta x}\right) \end{array} \right\} \tag{67}$$

And:

$$\lambda \to 1 \Rightarrow \left\{ \begin{array}{l} \sigma \to 1 \\ \omega \to 0 \end{array} \right\} \tag{68}$$

Note that as, according to Eq. (48), $(1-\sigma) \approx \Phi$ when $\lambda \to 1$, i.e.: $\sigma \approx 1 - \Phi = 1 - (1 = \lambda)^2$ when $\sigma \to 1$ that could help to determine λ from measurements of σ for big solutes. These measurements can consist in $\sigma = (\Delta p / RT \Delta c_s)_{J_v=0}$ as can be deduced from Eqs. (45) and (46). Note that $\omega = (J_s/RT\Delta c_s)_{J_V=0}$ tends to 0 when $\lambda \to 1$ It is worth noting that σ and ω have to be measured under carefully established experimental conditions according to these expressions and followed by extrapolation to zero gradients.

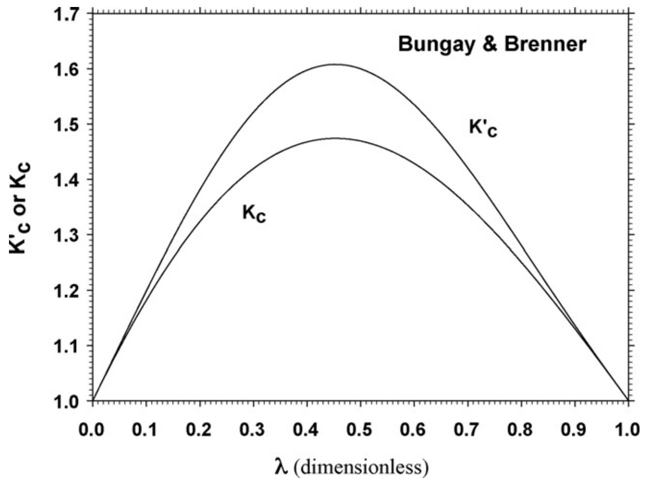

Fig. 3. The convective hindrance factor proposed by Bungay and Brenner with, K_c', and without, K_c, taking into account the effect of the pressure gradient, versus λ.

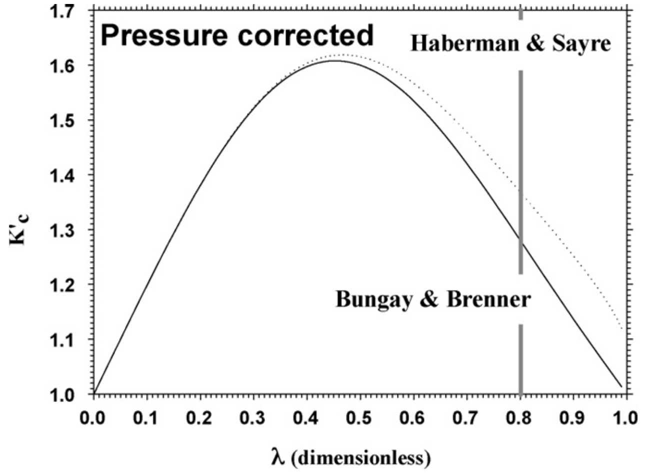

Fig. 4. The correlations of the convective hindrance factor versus λ proposed by Bungay and Brenner and Haberman y Sayre, both taking into account the effect of the pressure gradient.

In Figs. 1 and 2 it appears evident that among the correlations for the hindrance factors proposed in literature, those due to Brenner and Bungay are the only ones that perfectly adapt to the requirements above proved for both $\lambda \to 0$ and $\lambda \to 1$. Moreover, as shown in Figs. 3 and 4, the Bungay and Brenner correlation for the convective hindrance factor also shows correct limits for $\lambda \to 0$ and $\lambda \to 1$ when the effect of the applied pressure gradient is taken into account. In Fig. 5 the variation, in percentage, of the convective hindrance factor for negligible and non-negligible applied pressure gradients is shown versus λ. Note that the maximal increment in the hindrance factor, when the applied pressure gradient is taken into account, appears at $\lambda \approx 0.45$.

3. Resolution of transport equations

According to Eq. (40) and using that $J_s = c_{sp} J_V$ with c_{sp} the permeate concentration outside the membrane

$$\frac{dc_s(x)}{dx} = \frac{1}{A_K D_S}\left[\frac{K_c'}{K_d} c_s(x) - \frac{1}{\Phi K_d} c_{sp}\right] J_V \tag{69}$$

This equation can be integrated from the concentration at the pore entrances, c_{sf}, to the permeate concentration (at the pore end-

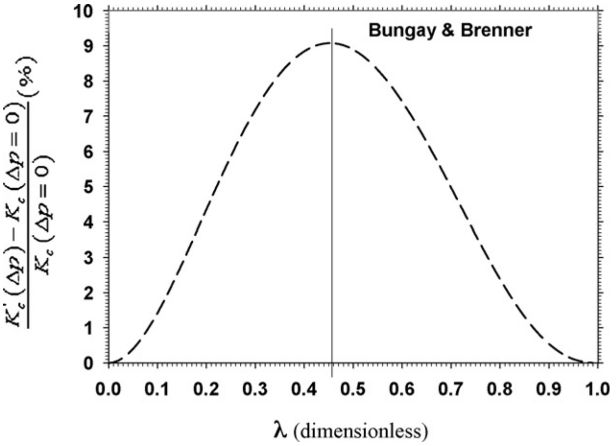

Fig. 5. Percentual variation of the convective hindrance factor versus λ when the effect of the pressure gradient is taken into account. The maximum corresponding to $\lambda \approx 0.45$, is shown by a line.

ing), c_{sp}, and used to evaluate the actual retention coefficient:

$$R_s' \equiv 1 - \left(\frac{c_{sp}}{c_{sf}}\right) = 1 - \frac{K_c'\phi}{1-(1-K_c'\phi)e^{-Pe_s'}} \tag{70}$$

c_{sf} is the feed concentration. The prima meaning that it includes the effect of the pressure gradient. The dimensionless Peclet number is then given by

$$Pe_s' = \frac{K_c' J_V}{K_d D_s}\left(\frac{\Delta x}{A_k}\right) \tag{71}$$

It is important to note that this Peclet number is not exactly the same as when the pressure gradient correction was not taken into account. It is, in any case, the ratio of convective to diffusive terms in the transport equation. Therefore it is the actual Peclet number, nevertheless we distinguish it from Pe_s that should include K_c instead of K_c'.

Eq. (70) states that R_s' is a function of J_V with r_p (included in Φ) and $\Delta x/A_k$ as parameters to be fitted. Nevertheless, according with the Hagen–Poiseuille model, for pure water:

$$\left(\frac{\Delta x}{A_k}\right) = \frac{1}{L_{pw}}\left(\frac{r_p^2}{8\eta_w}\right) \tag{72}$$

with L_{pw} the pure water permeability. Thus Eq. (71) can be written as:

$$Pe_s' = \frac{1}{D_s L_{pw}}\left(\frac{K_c' r_p^2}{K_d 8\eta_w}\right) J_V \tag{73}$$

On the other hand, inside a pore, as those typically appearing in nanofiltration membranes, which are similar in size to the water molecules adsorbed on the pore walls ($d_w = 0.28$ nm), the viscosity could go from the bulk value in the center of the pore to a value 10 times bigger at the pore walls. Thus, a profile can be assumed [12], as:

$$\frac{\eta_w}{\eta_0} = 1 + 18\left(\frac{d_w}{r_p}\right) - 9\left(\frac{d_w}{r_p}\right)^2 \tag{74}$$

being η_0 the bulk viscosity for pure water in non-restricted geometries. This augmented viscosity has to be used in Eq. (73) and thus in Eq. (70) to eliminate $\Delta x/A_k$, leaving r_p as the only fitting parameter to be obtained from experimental R_s versus J_V curves.

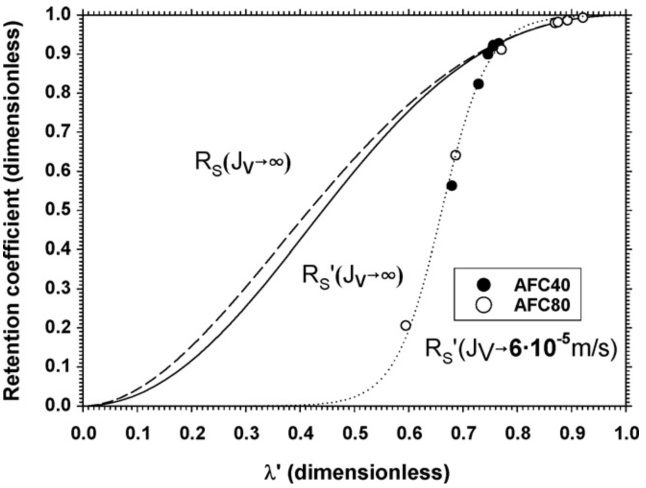

Fig. 6. Retention coefficients with, R_s', and without, R_s, taking into account the pressure gradient versus λ for volume flows extrapolated to infinity. Experimental results for the AFC-40 and AFC-80 membranes, for a high volume flow of $6{\cdot}10^{-5}$ m/s, are also shown.

On the other hand, according to Eq. (48), Eqs. (70) and (73) could be written as:

$$R_s' = \sigma\frac{1-e^{-Pe_s'}}{1-\sigma e^{-Pe_s'}} \tag{75}$$

and

$$Pe_s' = \frac{1-\sigma}{RT\omega} J_V \tag{76}$$

These equations should allow fitting experimental results of retention versus volume flow in terms of the two parameters σ and ω which are correlated with r_p according to Eqs. (48), (72) and (74). It is then clear that this is an alternative way of presenting the same process of evaluation.

4. Relevance of the pressure gradient

Eq. (70) can be extrapolated to $J_V \to \infty$ in order to evaluate easily and without the influence of a specific volume flow. This extrapolated true retention coefficient is the reflection coefficient, as shown in Eq. (48) [19]. This, without considering the pressure gradient, should lead to

$$\lim_{J_V\to\infty} R_s = 1 - K_c\phi = \sigma(\Delta p = 0) \tag{77}$$

And including the effect of the pressure gradient to

$$\lim_{J_V\to\infty} R_s' = 1 - K_c'\phi = \sigma(\Delta p \neq 0) \tag{78}$$

In Fig. 6 the retention coefficient neglecting the effect of the applied pressure gradient, R_s, and taking into account this pressure gradient, R_s', are shown as a function of λ for volume flows extrapolated to infinity thus being σ ($\Delta p = 0$) and $\sigma(\Delta p \neq 0)$.

As an example, the experimental results of retention versus molecular sizes [47,48], for two nanofiltration membranes made out of aromatic polyamide have been used. They are AFC80$^{\text{PCI}}$ and AFC40$^{\text{PCI}}$ (Paterson Candy International-Ltd., UK), made by the thin-film composite (TFC) method on a porous polysulfone substrate. According to the manufacturers, the recommended working temperature is below 60 °C, the maximum applied pressure is 6.0 MPa and pH must be in the 2–11 range.

The corresponding results for a constant high volume flow of $6{\cdot}10^{-5}$ m/s are also shown in terms of the pore radius relative to the solute radii as obtained from these experimental results [48],

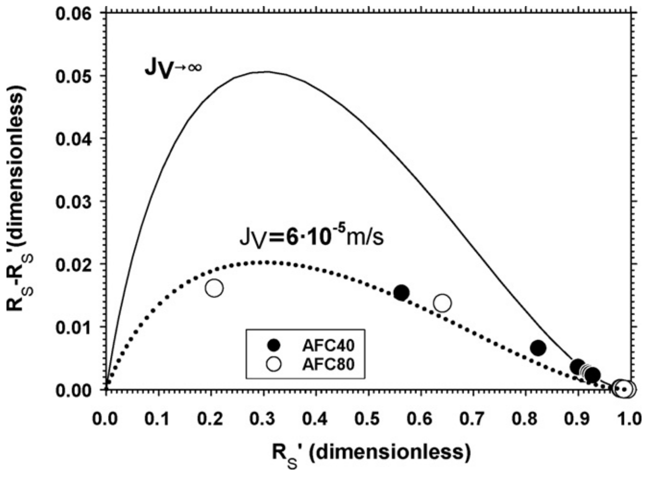

Fig. 7. Difference in retention coefficients with and without taking into account the pressure gradient versus the retention coefficient $R_s{}'$ for volume flows extrapolated to infinity. Experimental results for the AFC-40 and AFC-80 membranes are also shown. The corresponding dotted curve is only an eye-guide.

by assuming the applied pressure gradient as relevant. This size ratio can be called λ'; thus, it is $R_s{}'$ what is shown for these membranes. From these λ', the corresponding theoretical R_s coefficients can be easily evaluated, but they are not shown because they don not separate appreciably from the points shown.

Note that for highly retentive membranes, retention and reflection coefficients coincide as should be expected. As far as in these conditions the membrane should approach a prefect semipermeable membrane. In these conditions the effect of the pressure gradient and volume flow are also very small.

The relative change in the retention coefficient by taking into account the applied pressure gradient is also shown in Fig. 7. For the $J_V \to \infty$ extrapolation we also have:

$$\sigma(\Delta p = 0) - \sigma(\Delta p \neq 0) = \lim_{J_V \to \infty} \left(R_s - R_s{}'\right) = \left(K_c{}' - K_c\right) \phi \tag{79}$$

This theoretical curve for J_V extrapolated to infinity can be accepted as an upper limit for these deviations as can be seen in Fig. 7. In these limit conditions, it can be concluded that the changes in retention should be below a 5% being lower for relatively low and high retentions. As far as the AFC-40 and AFC-80 are very typical nanofiltration membranes, these errors should be probably for most of the cases below the 2% shown by these AFC membranes. In any case, these errors should increase for increasing membrane permeability.

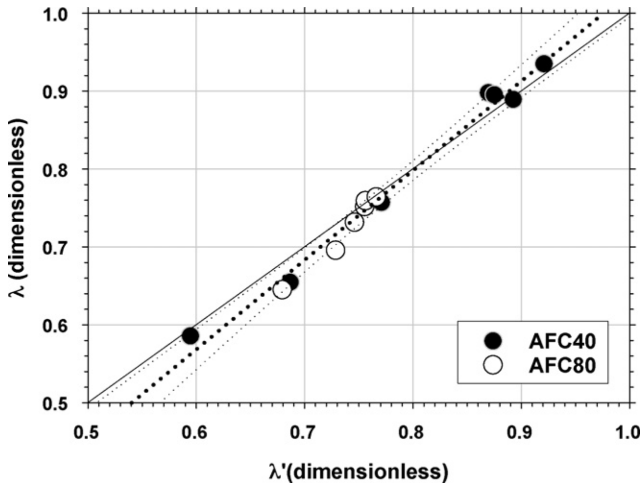

Fig. 8. λ as obtained by fitting experimental results for AFC-40 and AFC-80 membranes and assuming there is not an appreciable influence of the applied pressure versus λ′ as obtained by assuming that the pressure gradient has to be taken into account. The solid line corresponds to the hypothetical identity of λ and λ′. The dotted lines are the fitted line and the 95% confidence lines.

Finally in Fig. 8 the values for the pore radius relative to the solute radii as obtained from the experimental results for AFC-40 and AFC-80 by assuming that the applied pressure gradient as relevant, λ', and as negligible, λ, are shown. Note that there are not significant differences at least for relatively high solute sizes.

5. Conclusions

We have shown, in detail, how the usual model for the transport of neutral solutes through porous membranes, lead to equations that can be compared with the thermodynamic equations of transport. We focus in the assumptions used in the process of modeling and specifically we have shown that the model applies for diluted solutions of spherical molecules. On the other hand, when the hindrance factors are considered, its dependence on the ratio of molecular and pore radii is evaluated also for a low number of spherical molecules of the solute moving along the centerline of straight pores. We center our attention on cylindrical pores but this is not fundamental for the model, other correlations are proposed for example for slit pores.

In these conditions we show the total equivalence of using σ and ω as parameters or using r_p and $\mathrm{A_k}/\Delta\mathrm{x}$ as parameters to fit experimental results of retention versus volume flow. It is also equivalent to measure adequate and separately σ and ω and use their correlation with r_p and $A_k/\Delta x$ to evaluate them. In any case an adequate consideration of the amplification of viscosity in small pores is crucial. Moreover, it is also very convenient to use the Hagen–Poiseuille equation to eliminate $A_k/\Delta x$ in terms of the pure water permeability. It is worth noting, that σ and ω but also the retention coefficient have to be measured by taking into account the concentration polarization. Thus, in particular all the retention coefficients mentioned here refer to true retention rather than to observed retention.

Finally, we have shown that if the pore reflection coefficient is considered, the best pore hindrance correlation is that proposed by Bungay and Brenner. Nevertheless the influence in the retention coefficient or the reflection coefficient of the membrane system is limited with much higher relevance of the pore wall friction and applied pressure gradient. Inappropriately neglecting these contributions may lead to very significant errors in the prediction of performances of nanofiltration membranes, mainly for intermediate retentions.

Acknowledgements

Authors would like to thank Ministerio de Educación y Ciencia-Plan Nacional de I + D + i (Spain) (projects, CTQ2006-13012/PPQ and MAT2005-04976) and Junta de Castilla y León (VA116/A06, VA088A08 and ITACYL-BU-03-C3-2).

References

[1] W.S.W. Ho, K.K. Sirkar, Membrane Handbook, Van Nostrand Reinhold, New York, USA, 1992.
[2] N. Hilal, H. Al-Zoubi, N.A. Darwish, A.W. Mohamma, M. Abu Arabi, A comprehensive review of nanofiltration membranes: treatment, pretreatment, modelling, and atomic force microscopy, Desalination 170 (2004) 281–308.
[3] M.P.G. Muñoz, R. Navarro, I. Saucedo, M. Avila, P. Prádanos, L. Palacio, F. Martínez, A. Martín, A. Hernández, Hydrofluoric acid treatment for improved performance of a nanofiltration membrane, Desalination 191 (2006) 273–278.
[4] W.R. Bowen, H. Mukhtar, Characterisation and prediction of separation performance of nanofiltration membranes, J. Membr. Sci. 112 (1996) 263–274.

[5] A. Gamze, Modelling and Simulation of Nanofiltration Membranes, Cuvillier Verlag, Hamburg, Germany, 2007.

[6] J.A. Otero, G. Lena, J.M. Colina, P. Prádanos, F. Tejerina, A. Hernández, Characterisation of nanofiltration membranes—structural analysis by the DSP model and microscopical techniques, J. Membr. Sci. 279 (2006) 410–417.

[7] M.P. González, I. Saucedo, R. Navarro, P. Prádanos, L. Palacio, F. Martínez, A. Martín, A. Hernández, Effect of phosphoric and hydrofluoric acid on the structure and permeation of a nanofiltration membrane, J. Membr. Sci. 281 (2006) 177–185.

[8] M.P. González, I. Saucedo, R. Navarro, P. Prádanos, L. Palacio, F. Martínez, A. Martín, A. Hernández, Effect of phosphoric and hydrofluoric acid on the charge density of a nanofiltration membrane, Desalination 200 (2006) 361–363.

[9] R.R. Navarro, M.P. Gonzalez, I. Saucedo, M. Avila, P.P. Prádanos, F. Martínez, A. Martín, Hernández, Effect of an acidic treatment on the chemical and charge properties of a nanofiltration membrana, J. Membr. Sci. 307 (2008) 136–148.

[10] B. Van der Bruggen, C. Vandecasteele, Removal of pollutants from surface water and groundwater by nanofiltration: overview of possible applications in the drinking water industry, Environ. Pollut. 122 (2003) 435–445.

[11] B. Van der Bruggen, C. Vandecasteele, Modelling of the retention of uncharged molecules with nanofiltration, Water Res. 36 (2002) 1360–1368.

[12] W.R. Bowen, J.S. Welfoot, Modelling the performance of membrane nanofiltration—critical assessment and model development, Chem. Eng. Sci. 57 (2002) 1121–1137.

[13] A. Morão, M.T. Pessoa de Amorim, A. Lopes, I. Escobar, J.A. Queiroz, Characterisation of ultrafiltration and nanofiltration membranes from rejections of neutral reference solutes using a model of asymmetric pores, J. Membr. Sci. 319 (2008) 64–75.

[14] S.I. Nakao, S. Kimura, Models of membrane transport phenomena and their applications for ultrafiltration data, J. Chem. Eng. Jpn. 15-3 (1982) 2000–2005.

[15] W. Li, J. Li, T. Chen, Z. Zhao, C. Chen, Study of nanofiltration for purifying fructo-oligosaccharides II. Extended pore model, J. Membr. Sci. 258 (2005) 8–15.

[16] V. Silva, P. Prádanos, L. Palacio, A. Hernández, Alternative hindrance factors. What should be used for nanofiltration modelisation?, Desalination, submitted for publication.

[17] K.S. Spiegler, Transport processes in ionic membranes, Trans. Faraday Soc. 54 (1958) 1409–1428.

[18] O. Kedem, A. Katchalsky, A physical interpretation of the phenomenological coefficients of membrane permeability, J. Gen. Physiol. 45 (1961) 143–179.

[19] K.S. Spiegler, O. Kedem, Thermodynamics of hyperfiltration (reverse osmosis): criteria for efficient membranes, Desalination 1 (1966) 311–326.

[20] O. Kedem, V. Freger, Determination of concentration dependent transport coefficients in nanofiltration: defining an optimal set of coefficients, J. Membr. Sci. 310 (2008) 586–593.

[21] A. Verniory, R. Du Bois, P. Decoodt, J.P. Gassee, P.P. Lambert, Measurement of the permeability of biological membranes. Applications to the glomerular wall, J. Gen. Physiol. 62 (1973) 489–507.

[22] O. Kedem, A. Katchalsky, Thermodynamic analysis of the permeability of biological membranes to non-electrolytes, Biochem. Biophys. Acta 27 (1958) 229–246.

[23] X.L. Wang, T. Tsuru, M. Togoh, S. Nakao, S. Kimura, Transport of organic electrolytes with electrostatic and steric-hindrance effects though nanofiltration membranes, J. Chem. Eng. Jpn. 23 (1995) 372–380.

[24] X.L. Wang, T. Tsuru, S. Nakao, S. Kimura, The electrostatic and steric-hindrance model for the transport of charged solutes through nanofiltration membranes, J. Membr. Sci. 135 (1997) 19–32.

[25] B. Van der Bruggen, J. Chaep, D. Wilms, C. Vandecasteele, A comparison of models to describe the maximal retention of organic molecules in nanofiltration, Sep. Sci. Technol. 35 (2000) 169–182.

[26] J.W. Deen, Hindered transport of large molecules in liquid-filled pores, AIChE J. 33–9 (1987) 1409–1425.

[27] J.D. Ferry, Statistical evaluation of sieve constants in ultrafiltration, J. Gen. Physiol. 20 (1936) 95–104.

[28] J.R. Pappenheimer, E.M. Renkin, L.M. Borrero, Filtration, diffusion and molecular sieving through peripherical capillary membranes, Am. J. Physiol. 167 (1951) 13–46.

[29] E.M. Renkin, Filtration, diffusion and molecular sieving though porous cellulose membranes, J. Gen. Physiol. 38 (1954) 225–243.

[30] W.L. Haberman, R.M. Sayre, David Taylor Model Basin Report No. 1143, Washington, DC, US, Navy Dept., 1958.

[31] T. Bohlin, On the drag on rigid spheres, moving in a viscous liquid inside cylindrical tubes, Trans. Roy. Inst. Technol. (Stockholm) 155 (1960) 1–63.

[32] P.M. Bungay, H. Brenner, The motion of a closely fitting sphere in a fluid-filled tube, Int. J. Multiph. Flow 1 (1973) 25–56.

[33] J.L. Anderson, J.A. Quinn, Ionic mobility in microcapillaries. A test for anomalous water structures, J. Chem. Soc. Faraday Trans. I 68 (1972) 744–748.

[34] H. Brenner, L.J. Gaydos, The constrained Brownian movement of spherical particles in cylindrical pores of comparable radius, J. Colloid Interface Sci. 58 (1977) 312–356.

[35] G.M. Mavrovouniotis, H. Brenner, Hindered sedimentation and dispersion coefficients for rigid, closely fitting Brownian spheres in circular cylindrical pores containing quiescent fluids, Paper No. 85b, AIChE Ann. Meet., Miami, USA, 1986.

[36] W.R. Bowen, A.O. Sharif, Transport through microfiltration membranes: particle hydrodynamics and flux reduction, J. Colloid Interface Sci. 168 (1994) 414–421.

[37] W.R. Bowen, A.W. Mohammad, N. Hilal, Characterisation of nanofiltration membranes for predictive purposes—use of salts, uncharged solutes and atomic force microscopy, J. Membr. Sci. 126 (1997) 91–105.

[38] S. Bandini, D. Vezzani, Nanofiltration modeling: the role of dielectric exclusion in membrane characterization, Chem. Eng. Sci. 58 (2003) 3303–3326.

[39] M.G. Davidson, W.M. Deen, Hydrodynamic theory for the hindered transport of flexible macromolecules in porous membranes, J. Membr. Sci. 35 (1988) 167–192.

[40] J.C. Giddings, E. Kucera, C.P. Russell, M.N. Myers, Statistical theory for the equilibrium distribution of rigid molecules in inert porous networks. Exclusion chromatography, J. Phys. Chem. 72 (1968) 4397–4408.

[41] R.G. Priest, Integral-equation method for calculating entropy of confined chains, J. Appl. Phys. 52 (1981) 5930–5933.

[42] M. Meireles, A. Bessieres, I. Rogissart, P. Aimar, V. Sánchez, An appropriate molecular size parameter for porous membranes calibration, J. Membr. Sci. 103 (1995) 105–115.

[43] W.M. Deen, C.R. Bridges, B.N.M. Brenner, B.D. Myers, Hetero-porous model of glomerular size-selectivity: application to normal and nephritic humans, Am. J. Physiol. 249 (1985) F374–F573.

[44] P. Dechadilok, W.M. Deen, Hindrance factors for diffusion and convection in pores, Ind. Eng. Chem. Res. 45 (2006) 6953–6959.

[45] J.J.L. Higdon, G.P. Muldowney, Resistance functions for spherical particles, droplets and bubbles in cylindrical tubes, J. Fluid. Mech. 298 (1995) 193–210.

[46] J. Ennis, H. Zhang, G. Stevens, J. Perera, P. Scales, S. Carnie, Mobility of protein through a porous membrane, J. Membr. Sci. 119 (1996) 47–58.

[47] J.A. Otero, R. Gutiérrez, I. Arnaez, P. Prádanos, L. Palacio, A. Hernández, Structural and functional study of two nanofiltration membranes, Desalination 200 (2006) 354–355.

[48] J.A. Otero, O. Mazarrasa, J. Villasante, V. Silva, P. Prádanos, J.I. Calvo, A. Hernández, Three independent ways to obtain information on pore size distributions of nanofiltration membranes, J. Membr. Sci. 309 (2008) 17–27.